

Patterned Growth of TiO₂ Nanowires on Titanium Substrates

Jong-Yoon Ha^{1,2}, Brian D. Sosnowchik¹, Liwei Lin¹, Dong Heon Kang³, and Albert V. Davydov^{2*}

¹Berkeley Sensor and Actuator Center, Department of Mechanical Engineering, University of California at Berkeley, CA 94720, U.S.A.

²National Institute of Standards and Technology, Gaithersburg, MD 20899, U.S.A.

³Department of Electronic Materials Engineering, The University of Suwon, Suwon 445-743, Korea

Received March 9, 2011; accepted April 29, 2011; published online May 20, 2011

Single-crystalline rutile TiO₂ nanowires (NWs) were synthesized by the vapor–liquid–solid (VLS) method on Ti foil substrates patterned with catalytic Sn nano-islands. NWs of 3 to 8 μm in length and 50 to 500 nm in diameter were grown along the [110] axis exhibiting a rectangular cross section with the (001) and (110) side facets. This facile approach to TiO₂ NW fabrication with fast induction heating and short processing time utilizes the Ti foil both as a substrate and as a metal supply, thus eliminating the need for a separate titanium source.

© 2011 The Japan Society of Applied Physics

Nanostructured TiO₂ has versatile chemical, electrical, optical, and mechanical properties that are important for application in catalysis,¹ optical devices,² gas and humidity sensors,^{3,4} solar cells,⁵ Li-ion batteries,⁶ and biomedical materials.⁷ TiO₂ nanowires (NWs) can be synthesized by a variety of wet chemistry and vapor transport methods. Adachi *et al.* have reported the synthesis of titania NWs using hydrothermal reactions in the presence of micelles.⁸ The fabrication of TiO₂ NWs by the direct oxidation of titanium substrates⁹ and chemical vapor deposition (CVD)^{10,11} including metal–organic CVD¹² has also been reported. However, these methods typically require complex setups and processes, harsh environmental conditions, and extended processing times.

We have recently reported the fabrication of nanostructures such as carbon nanotubes,¹³ zinc oxide NWs,¹⁴ and TiO₂ nano-“swords”¹⁵ in an inductively heated system. The vapor–liquid–solid (VLS)¹⁴ and the vapor–solid (VS)¹⁵ growth mechanisms have been successfully realized to fabricate high-quality oxide NWs with extremely short heating times. In this study, we utilized the metal-catalyst VLS method in an inductively heated reactor to synthesize TiO₂ NWs on a Ti foil substrate patterned with Sn nano-islands. In this facile approach, the reactive Ti and O-containing species were supplied by the titanium substrate and residual oxygen from the carrier gas, respectively.

The growth process started with the deposition of a 200-nm-thick titanium layer by thermal evaporation onto a 0.5-mm-thick, 5 × 5 mm² Ti foil, followed by thermal evaporation of a 50-nm-thick Sn film using a transmission electron microscopy (TEM) grid as a shadow mask to create a periodic array of 70 × 70 μm² square patterns. The Sn-patterned Ti substrate was placed on a susceptor inside the induction heating system described in ref. 15. After the quartz chamber was evacuated to 250 mTorr, Ar with 2% H₂ (99.99% purity) was introduced into the system through a mass-flow controller. Upon reaching 1 atm, the gas flow was terminated and the sample was subjected to inductive heating. After reaching 850 °C within 10 s (as monitored by optical pyrometry), the process temperature was held for 10 min followed by a power-off cooling process.

The crystal structure of the fabricated TiO₂ NWs was analyzed by X-ray diffraction (XRD) and high-resolution transmission electron microscopy (HRTEM). The shapes,

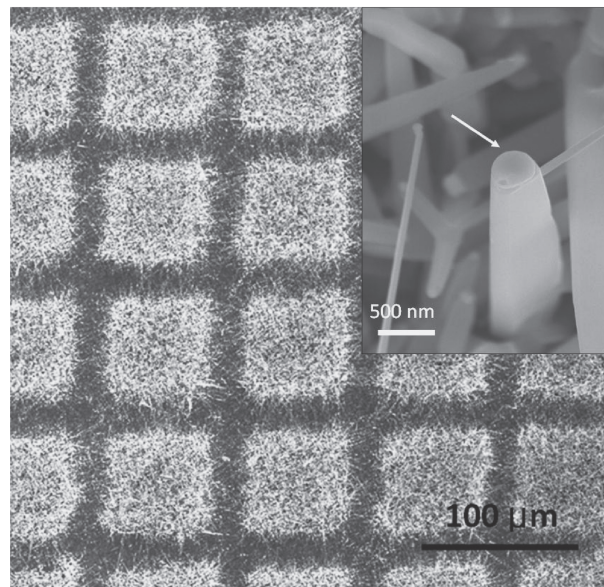


Fig. 1. Plan-view SEM image of periodic array of TiO₂ NWs fabricated on Ti foil. The Sn-based cap is clearly visible atop the NW (marked with arrow) in the inset, indicating the VLS growth mechanism.

composition, and microstructure of NWs were characterized by field-emission scanning electron microscopy (FESEM), equipped with X-ray energy dispersive spectroscopy (X-EDS) and electron backscatter diffraction (EBSD).

Figure 1 shows an array of TiO₂ NWs fabricated on titanium foil. NWs grew selectively within the Sn-patterned squares, clearly demonstrating the catalytic effect of tin on the growth process. The lengths of the NWs varied from 3 to 8 μm, and their diameters varied from 50 to 500 nm. The high-magnification SEM (Fig. 1, inset) image shows a representative NW of rectangular prismatic shape with the solidified catalytic droplet atop. X-EDS elemental analysis confirmed that the droplets were tin-based, while the NWs were composed of titanium and oxygen (33 ± 2 at. % Ti and 67 ± 2 at. % O, which corresponds to the TiO₂ stoichiometry). Microstructural EBSD analysis (Fig. 2) substantiated the X-EDS results: the catalytic caps had β-Sn structure and the NWs were single crystals with rutile structure. According to EBSD, the NW growth direction was along the [110] axis and the prismatic side facets were (001) and (110) planes. TEM analysis (not shown) verified the NW growth axis and facet identification and indicated that the NWs were virtually free of structural defects.

*E-mail address: albert.davydov@nist.gov

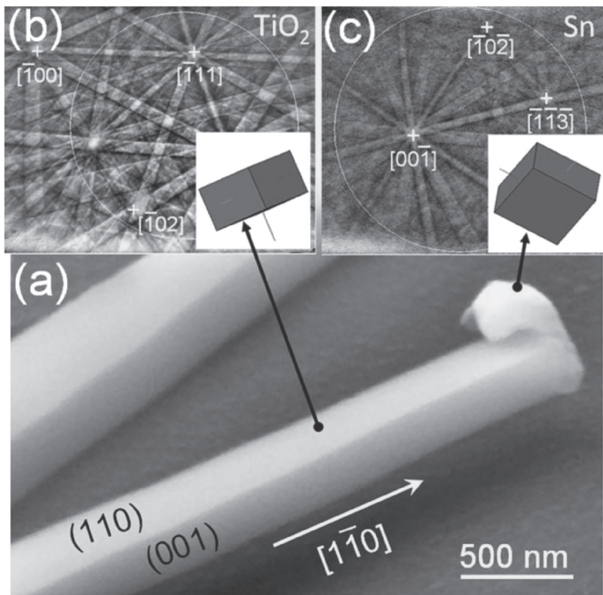


Fig. 2. (a) SEM image, (b) and (c) corresponding EBSD patterns of the TiO₂ NW and catalytic Sn cap, respectively. Insets in diffraction patterns (b) and (c) are simulated crystallographic orientations of TiO₂ and Sn unit cells, respectively.

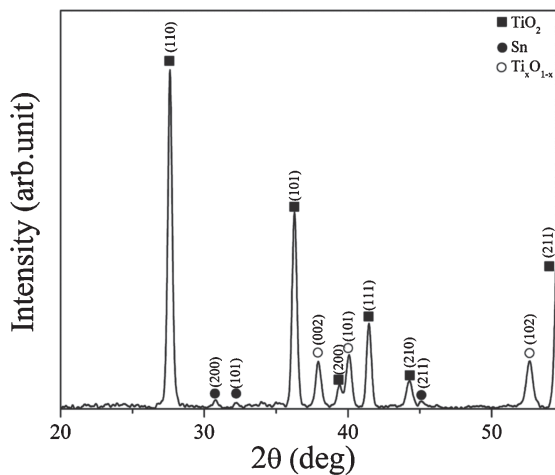


Fig. 3. XRD pattern of TiO₂ NWs on Ti substrate. Rutile peaks (filled squares) correspond to both NWs and the TiO₂ layer formed on the substrate (see “layer A” in Fig. 4). Sn peaks (filled circles) correspond to catalytic metal caps residing atop NWs. Ti_{1-x}O_x peaks (open circles) are from the oxidized titanium substrate (“layer B” in Fig. 4).

XRD (Fig. 3) revealed the presence of three phases in the sample shown in Fig. 1: rutile TiO₂, β -Sn, and a hexagonal phase. The presence of the first two phases, titania ($P42/mnm$; $a = 0.4584 \pm 0.0002$ nm, $c = 0.2955 \pm 0.0001$ nm) and tin ($I41/amd$; $a = 0.5830 \pm 0.0003$ nm, $c = 0.3179 \pm 0.0002$ nm), was expected because of the EBSD and TEM analyses of the NWs and agreed well with the reference XRD data.^{16,17} The third phase was identified as Ti-based hcp $P63/mmc$ and was thought to come from the titanium substrate. However, its experimental lattice parameters ($a = 0.2958 \pm 0.0005$ nm, $c = 0.4756 \pm 0.0006$ nm) were significantly larger than those of pure titanium ($a =$

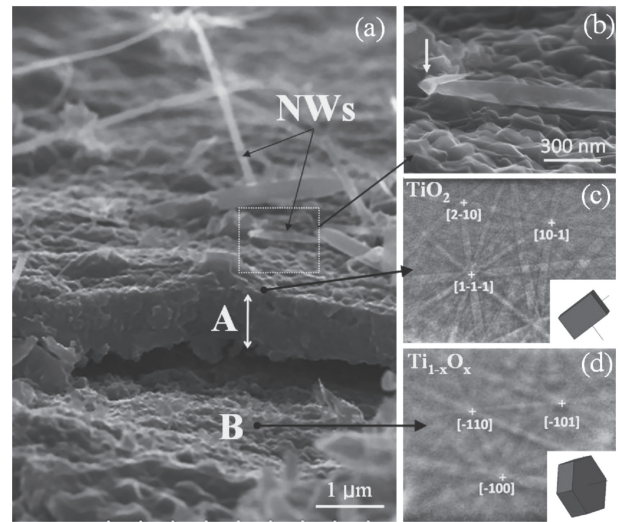


Fig. 4. (a) SEM perspective view of sample from Fig. 1: TiO₂ NWs grow on “layer A”, which delaminated from “layer B” (note that NWs were partially removed for a clear view of surfaces and interfaces); (b) close-up view of NW with arrow pointing to Sn-cap; (c) and (d) EBSD patterns of “layer A” (TiO₂) and “layer B” (Ti_{1-x}O_x), respectively.

0.2950 nm, $c = 0.4686$ nm¹⁸), suggesting the formation of a Ti_{1-x}O_x phase due to the dissolution of oxygen in the titanium foil. Based on the known compositional dependence of lattice parameters for the Ti_{1-x}O_x solid solution,¹⁸ the x value was calculated to be 0.19 ± 0.03 (i.e., 81 ± 3 at.% Ti and 19 ± 3 at.% O). The dissolution of oxygen in the substrate during growth was verified by point-to-point microstructural EBSD and compositional X-EDS analyses on a cross-sectional sample from Fig. 1. The perspective SEM view of such a sample in Fig. 4(a) revealed two distinct layers underneath the NWs. It can be seen that the top 1- μ m-thick “layer A” was partially delaminated from the adjacent thick substrate “layer B”. Cross-sectional X-EDS line scan (not shown) identified “layer A” as having 34 ± 2 at.% Ti and 66 ± 2 at.% O (i.e., close to TiO₂ stoichiometry), while the adjacent *ca.* 250- μ m-thick “layer B” had an average composition of 82 ± 2 at.% Ti and 18 ± 2 at.% O. EBSD analysis of the top surfaces of both layers identified “layer A” as the TiO₂ rutile phase [Fig. 4(b)] and the adjacent substrate “layer B” as the hcp $P63/mmc$ phase [Fig. 4(c)]. The SEM/EBSD results explain the XRD results in Fig. 3: the TiO₂ peaks (filled squares in Fig. 3) are reflections from both NWs and “layer A”, while the Ti_{1-x}O_x peaks (open circles in Fig. 3) are from the partially oxidized “layer B”. Thus, SEM, EBSD, and XRD consistently describe the final product microstructure, which consisted of single-crystalline TiO₂ NWs that grew on top of a 1- μ m-thick TiO₂ polycrystalline layer, which in turn resided on the Ti_{1-x}O_x ($x = 0.19 \pm 0.03$) substrate layer.

A schematic diagram of the growth process is given in Fig. 5, and can be summarized as follows: the Sn-coated Ti substrate reacts at elevated temperatures with O₂ and forms three distinct products: (i) TiO₂ NWs, (ii) TiO₂ polycrystalline thin film (“layer A”), and (iii) Ti_{1-x}O_x partially oxidized titanium substrate (“layer B”). For (i),

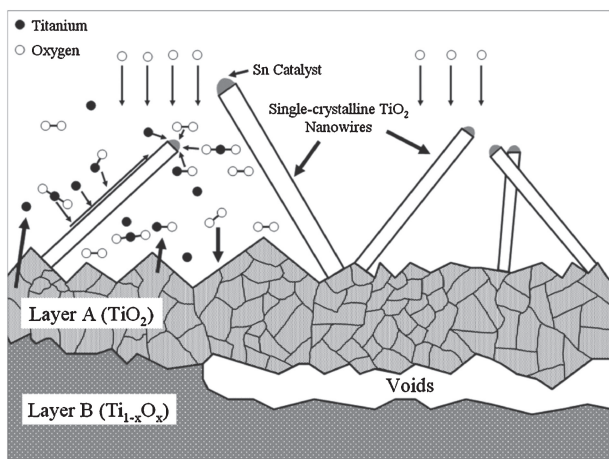


Fig. 5. Schematic diagram of the TiO_2 NW growth on Ti foil. For the NW growth, which occurs via the VLS mechanism, Ti-containing gas species are supplied by the foil itself, while oxygen is supplied by residual O_2 from the carrier gas. In addition to the NW growth, a 1- μm -thick polycrystalline TiO_2 layer (“layer A”) forms on top of the partially oxidized $\text{Ti}_{0.81}\text{O}_{0.19}$ layer (“layer B”).

NWs apparently grow via the VLS mechanism: molten tin islands, which form upon dewetting from titanium substrate, act as catalytic nucleation sites by absorbing O- and Ti-containing gas species with subsequent precipitation of TiO_2 NWs. Since NW diameter is defined by a catalytic droplet size, it explains a variation of NW diameters from tens to hundreds of nanometers due to a large span of tin islands sizes. Similarly, lateral distribution of NWs corresponded to the density of catalytic islands on the substrate. Note that the reactive oxygen likely comes in a miniscule amount from the carrier gas, while Ti-containing gas species, likely in the form of Ti, TiO, and TiO_2 molecules and associated ions,^{19,20} originate from the substrate itself and from its reaction with oxygen. For the reaction products (ii) and (iii), oxygen apparently diffuses directly into the substrate and forms $\text{Ti}_{1-x}\text{O}_x$ and TiO_2 phases. The formation of both layers is in good agreement with previously reported titanium oxidation experiments, in which two distinct processes take place: oxygen dissolution and “rutile-scale” formation.^{21–23} While there were no *in-situ* growth and observation experiments here, it is reasonable to assume that the NW growth (i) proceeds in parallel with the substrate oxidation processes (ii) and (iii).

In conclusion, single-crystalline rutile TiO_2 NWs were fabricated by the tin-catalyst assisted VLS method in an inductively heated CVD reactor. Patterned titanium substrates served as a source of Ti-containing reactive species, while residual oxygen was supplied from the ambient gas in the reactor. Sn-capped TiO_2 NWs were 3 to 8 μm in length and 50 to 500 nm in diameter. The NWs had a rectangular cross section with (110) and (001) side facets and grew along the $[1\bar{1}0]$ axis. This facile approach, with fast induction heating and a short processing time, in which the metal foil serves both as a substrate and as a material source for the oxide growth, could be readily applied for a variety of metal oxide NW fabrications.

Acknowledgment This work was partially supported by a Korea Research Foundation Grant funded by the Korean Government (MOEHRD): KRF-2007-357-D00120.

- 1) M. R. Hoffmann, S. T. Martin, W. Choi, and D. W. Bahnemann: *Chem. Rev.* **95** (1995) 69.
- 2) J. E. G. J. Wijnhoven and W. L. Vos: *Science* **281** (1998) 802.
- 3) I.-D. Kim, A. Rothschild, B. H. Lee, D. Y. Kim, S. M. Jo, and H. L. Tuller: *Nano Lett.* **6** (2006) 2009.
- 4) O. K. Varghese, D. Gong, M. Paulose, K. G. Ong, E. C. Dickey, and C. A. Grimes: *Adv. Mater.* **15** (2003) 624.
- 5) B. O'Regan and M. Gratzel: *Nature* **353** (1991) 737.
- 6) B. Liu, D. Deng, J. Y. Lee, and E. S. Aydil: *J. Mater. Res.* **25** (2010) 1588.
- 7) C. Cui, H. Liu, Y. Li, J. Sun, R. Wang, S. Liu, and A. L. Greer: *Mater. Lett.* **59** (2005) 3144.
- 8) M. Adachi, T. Harada, and M. Harada: *Langmuir* **16** (2000) 2376.
- 9) S. S. Amin, S.-Y. Li, X. Wu, W. Ding, and T. F. Xu: *Nanoscale Res. Lett.* **5** (2010) 338.
- 10) J. M. Wu, H. C. Shin, and W. T. Wu: *Chem. Phys. Lett.* **413** (2005) 490.
- 11) J.-C. Lee, K.-S. Park, T.-G. Kim, H.-J. Choi, and Y.-M. Sung: *Nanotechnology* **17** (2006) 4317.
- 12) S. K. Pradhan, P. J. Peucroft, F. Yang, and A. Dozier: *J. Cryst. Growth* **256** (2003) 83.
- 13) B. D. Sosnowchik and L. Lin: *Appl. Phys. Lett.* **89** (2006) 193112.
- 14) L. Luo, B. D. Sosnowchik, and L. Lin: *Appl. Phys. Lett.* **90** (2007) 093101.
- 15) B. D. Sosnowchik, H. C. Chiamori, Y. Ding, J.-Y. Ha, Z. L. Wang, and L. Lin: *Nanotechnology* **21** (2010) 485601.
- 16) Powder diffraction file™, International Centre for Diffraction Data, Newtown Square, PA, 1998, 86-0148.
- 17) Powder diffraction file™, International Centre for Diffraction Data, Newtown Square, PA, 1998, 86-2265.
- 18) S. Andersson, B. Collén, U. Kuylenstierna, and A. Magnéli: *Acta Chem. Scand.* **11** (1957) 1641.
- 19) W. O. Grovesm, M. Hoch, and H. L. Johnston: *J. Phys. Chem.* **59** (1955) 127.
- 20) P. W. Gillers, K. D. Carlson, H. F. Franzen, and P. G. Wahlbeck: *J. Chem. Phys.* **46** (1967) 127.
- 21) P. Kofstad: *J. Less-Common Met.* **12** (1967) 449.
- 22) J. E. Lopes Gomes and A. E. Huntz: *Oxid. Met.* **14** (1980) 249.
- 23) P. K. Imbrie and D. C. Lagoudas: *Oxid. Met.* **55** (2001) 359.